PCCP

Accepted Manuscript

ROYAL SOCIETY OF CHEMISTRY

www.rsc.org/pccp

Journal Name

ARTICLE TYPE

Cite this: DOI: 10.1039/xxxxxxxxxx

Self Assembly of Phospholipids on Flat Supports†

Anil R. Mhashal,*[a] and Sudip Roy*[a]

Received Date
Accepted Date

DOI: 10.1039/xxxxxxxxxx

www.rsc.org/journalname

Current study deals with the self-assembly of the phospholipids on flat supports using Martini coarse grain model. We reported here the effect of hydrophilic and hydrophobic nature of the solid supports on the lipid self-assembly. The hydrophilic and hydrophobic supports were modeled on the basis of water droplet simulations. The present work addresses the self-assembly mechanism of lipids on eight different supports with different strength of hydrophilicity and hydrophobicity. We demonstrated how interplay between the interactions of lipid and water with the support can guide lipid self-assembly process. Thereafter, we calculated the energetics of the components of the system to quantify the competitions between water and lipid head-group with hydrophilic supports. Finally, the properties of the self-assembled bilayers were also analyzed and reported here.

1 Introduction

Recently, Supported lipid bilayers (SLBs) gained lot of attention due to its various applications in the areas of biological and pharmaceutical research.[1–3] Supported bilayer is used for studying the cell membrane as it preserves the functions and properties of the lipid bilayer as observed in living cells.[4–6] SLBs are excellent model to understand the T cell immunological synapse,[7,8] neuronal interactions,[9] and the triggering of EphA2 receptor in mammary epithelial cells.[10] The SLBs are also used as biosensors and biodevices.[6,11–13] Richter *et al.*[14] reviewed various SLB systems that includes solid-supported lipid bilayers,[15–19] polymer-cushioned lipid bilayers,[20–22] hybrid bilayers,[23,24] tethered lipid bilayers,[25] suspended lipid bilayers,[26,27] and supported vesicular layers.[28,29] Experimentally, the SLBs are formed on solid substrates like silica-based surfaces (e.g., glass, aerogels, xerogels) and mica.[1,30–32] Among the several experimental methods for the formation of SLBs[4], the vesicle fusion[33] and Langumuir-Blodgett[34,35] are considered as the most commonly used techniques to yield SLBs. However, theoretical studies dealt with SLB involve deposition of self-assembled lipid bilayer over solid substrate. One of the theoretical investigations of SLB was done by Xing *et al.*.[36] They performed molecular level simulations of free standing pre-assembled bilayer on the model supports. They transferred pre-assembled lipid bilayers in water to model supports which was further simulated by using molecular dynamics. The study emphasized on the properties of lipid bilayer as a function of geometry and chemical nature of the support.

The support essentially plays a vital role in determining the properties of supported membrane. The physical and chemical properties of the substrate often change the properties of deposited bilayer/monolayer such as decoupled phase transitions[37–40] and structural and dynamical heterogeneity of inner and upper leaflet.[41–43] Cha *et al.* showed that the surface charge density of support controls the rupture of adsorbed lipid vesicles to form stable, supported phospholipid bilayers.[44] Lin X. *et al.* investigated the interactions between hydrophilic nanoparticle with the bilayer supported on the surface.[45]

Self-assembly of the lipids on the supports can produce supported lipid bilayers alternative to the deposition of the pre-assembled lipid assemblies on supports. Besides that, the self assembly of lipids from the complete disordered state in the presence of artificial model surface is unexplored till date. Therefore, it would be interesting to understand the complex self-assembly process in the influence of the external perturbations due to supports. Hwankyu Lee[46] studied the self-assembly of lipids on single-walled carbon nanotube by performing molecular simulations. They performed simulations of lysophospholipids and phospholipids grafted/ungrafted with polyethylene glycol (PEG) and studied the assemblies of these lipids on the nanotube. They reported the formation of cylindrical monolayer resembling micelle of the di-palmityl-phosphotidylcholine (DPPC) and di-palmitoyl-phosphatidylglycerol (DPPG) lipids around the nanotube. The hydrophobic nature of the carbon nanotube induces the adsorption of the lipid in a monolayer fashion. However, on the other hand, the substrates used in case of SLBs are mostly hydrophilic in nature e.g., silica derivative substrates. The supported lipids on the such substrate maintain the bilayer morphology in head-tail-tail-head fashion with lipid head-groups facing hydrophilic support.[36,45] Hence after self-assembly, one could expect different macroscopic structure depending on the chemical nature of the substrate.

[a] *Physical Chemistry Division, National Chemical Laboratory, Pune, India. Fax: +9120 2590 2615; Tel: +9120 2590 3148; E-mail: ar.mhashal@ncl.res.in*

† Electronic Supplementary Information (ESI) available: [details of any supplementary information available should be included here]. See DOI: 10.1039/b000000x/

It is also reported that the chemical nature of the support has an effect on the bilayer properties.[36–43] It is believed that hydrophobic or hydrophilic nature of substrates can affect the bilayer properties differently. However, it is also probable that different strength of hydrophilicity or hydrophobicity of the support affects the bilayer properties to a different extent.

To the best of our knowledge, self-assembly simulations of lipids on flat surfaces having different hydrophobicity and hydrophilicity were not studied. Therefore, in our study, we have simulated self-assembly DPPC lipids on flat supports by varying the hydrophobicity and hydrophilicity to elucidate the mechanism of self-assembly. We have also analyzed and compared the properties of the self-assembled supported bilayers. The choice of the parameters to define hydrophilic or hydrophobic support was decided on the basis of the water droplet simulation on the model support. In the present work, we have constructed eight supports with different strengths of hydrophobicity and hydrophilicity and have employed molecular dynamics (MD) simulation to self-assemble the lipids on these supports. The present work is mainly focused on the following issues a) self-assembly lipids on flat support and b) effect of hydrophobic and hydrophilic nature of support on self-assembly of the lipids c) properties of the lipid bilayer on different support and d) the mechanism and energetics of lipid self-assembly process.

2 Computational Methods

All the simulations were carried out using GROMACS 4.5.5[47,48] simulation code. The coarse grained Martini model for lipid and water proposed by Marrink were used.[49–51] In this work, we have considered model solid supports made of hydrophilic and hydrophobic beads. The hydrophobicity and hydrophilicity of the support were decided on the basis of interaction strength (parameters) ε_{SW} between the support beads (S) and water (W) beads. Martini force field consists of 4 types of beads, polar (P), nonpolar (N), apolar (C) and charged (Q). The hydrophobic moieties in force field are represented as type C beads with five variants from C1 to C5. Type C1 bead is the most repulsive to water with interaction parameter $\varepsilon_{ij} = 2.0$ kJ/mol and the C5 bead ($\varepsilon_{ij} = 3.1$ kJ/mol) is relatively less hydrophobic in nature while hydrophilic P5 bead is most attractive ε_{ij}=5.6 kJ/mol bead among all beads. Therefore, we have constructed the hydrophobic and hydrophilic supports based on the above parameters and have checked their effect on water droplet. We have also modified the parameters to tune the hydrophobicity/hydrophilicity of these support beads and performed MD simulations of whole system consisting of the support, DPPC and water beads.

The non-bonded terms in the Martini force field are modeled by pairwise Lennard-Jones (LJ) interactions and cross terms σ_{ij} and ε_{ij} are defined by combination rule of geometric mean. The hydrophobic supports were constructed by considering the most hydrophobic bead. Type C1 is the most water repulsive bead in Martini force field, represented by $\varepsilon_{ij} = 2.0$ kJ/mol. We have constructed the support with beads with hydrophobicity more than C1 ($\varepsilon_{SW} < 2.0$ kJ/mol) beads (see Figure 1).

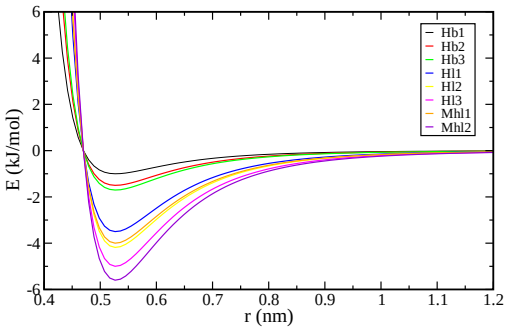

Fig. 1: Lennard Jones potential between water and surface beads. Colors black, red, green, blue, yellow, magenta, orange and violet represents systems Hb1, Hb2, Hb3, Hl1, Hl2, Hl3, Mhl1 and Mhl2 respectively

The strength and reliability of the hydrophobicity of the support was further checked by performing water droplet simulations. Water droplet simulations were performed on model support made of four layers of fixed particles (S) positioned on a square grid separated by 0.3 nm distance. This results in the adjacent support beads of 0.47 nm radius and diagonally placed beads to overlap on each other, hence leaving no gap in the support thereby not allowing any water bead to pass through it. However, the support-support bead interactions were turned off in all the simulations. The dimension of the support was 12.6 nm$\times$12.6 nm along the XY plane (details of which are explained in the following section). We have kept additional 0.3 nm of box dimension in both X and Y direction to maintain the periodicity of support beads without superimposition. A semi-hemispherical water droplets of 4580 water beads were then simulated on six different supports with $\varepsilon_{SW} = 1.0$ kJ/mol, $\varepsilon_{SW} = 1.5$ kJ/mol, $\varepsilon_{SW} = 1.7$ kJ/mol, $\varepsilon_{SW} = 1.8$ kJ/mol, $\varepsilon_{SW} = 2.0$ kJ/mol and $\varepsilon_{SW} = 5.0$ kJ/mol. The σ values for all the beads were chosen as 0.47 nm as in Martini force field. The droplet simulations were performed for 60 ns and wetting or dewetting of the supports were quantified by calculating the number of water beads coming in the contact (with in 1 nm from support) with the support surface as a function of simulation time (Figure S1 a of electronic supplementary material (ESI)).

The wetting of the support surface indicates the hydrophilic nature of the support beads and it is accounted from the number of the water beads in contact with support. Similarly, the lesser count of water in support surface contact indicates the hydrophobic nature of the support. The wetting of the support surface can also be visualized from the droplet spreading depicted in Figure S1 b. From Figure S1 a, we have shown that the supports with ε_{SW}= 1.0 kJ/mol (Hb1), ε_{SW}= 1.5 kJ/mol (Hb2) and ε_{SW}= 1.7 kJ/mol (Hb3) retains the droplet structure and does not wet the surface. A rise in the number of water beads near the support is observed beyond ε_{SW}= 1.7 kJ/mol which indicates the hydrophilic nature of supports. Hence beads with ε_{SW}= 1.0, 1.5 and 1.7 kJ/mol were considered as hydrophobic and used to construct the support for lipid self-assembly simulations. The final snapshots of the water droplets simulations are depicted in Figure S1 b for hydrophobic supports which are denoted as Hb1 (ε_{SW} = 1), Hb2 (ε_{SW}=1.5) and Hb3 (ε_{SW}= 1.7). Moreover, we

have also constructed the supports with support-water interaction parameter (ε_{SW}) higher than of hydrophobic (ε_{C1W}) interactions in Martini force field.[49–51] The supports are hydrophilic in nature due to the ε_{SW} used and as confirmed from the droplet simulations (See Figure S1 a). These hydrophilic supports are denoted as Hl1 (ε_{SW} = 3.5 kJ/mol), Hl2 (ε_{SW} = 4.18 kJ/mol) and Hl3 (ε_{SW} = 5 kJ/mol), where Hl3 is the most hydrophilic systems considered here. The surface-water interactions are carefully chosen for all hydrophobic and hydrophilic systems except Mhl1 and Mhl2 (described below) (Table 1) which are taken from Martini.

Table 1: Non-bonded interaction strength (ε_{ij} in kJ/mol) between the particles.

System	Surface-Water	Surface-Head	Surface-Tail	Head-Head	Tail-Tail
Hb1	1.0	0.83	0.83	3.5	3.5
Hb2	1.5	1.25	1.25	3.5	3.5
Hb3	1.7	1.42	1.42	3.5	3.5
Hl1	3.5	2.92	2.92	3.5	3.5
Hl2	4.18	3.5	3.5	3.5	3.5
Hl3	5.0	4.18	4.18	3.5	3.5
Mhl1	4.0	4.0	2.0	3.5	3.5
Mhl2	5.6	5.0	2.0	3.5	3.5

For Mhl1 and Mhl2 we have used Nda and P5 types of Martini beads which are commonly used to represent hydrophilic support in supported lipid bilayer simulations. Lin X. *et al.* have studied the properties of the lipid membrane on the hydrophilic support made of Nda type beads.[45] In the present study, the Nda type surface bead is represented as Martini hydrophilic bead (Mhl1). Additionally we have considered P5 beads to represent the most hydrophilic Martini support (ε_{SW} =5.6 kJ/mol) and termed as system Mhl2. It exhibits higher interactions with water compared to rest of the beads. Hence, as described above in total we have constructed eight systems with different model supports based on the interaction with water beads ε_{SW} ranging from 1.0 kJ/mol to 5.6 kJ/mol given in the Table 1 and as depicted in Figure 1.

The interaction between the support and the rest of the beads was carefully parameterized. Initially, we have calculated the interaction parameters (ε_{SS}) from the desired ε_{SW} by solving the geometric mean combination rule (equation 1). Further, the interactions of the surface beads with other beads are calculated e.g., interactions between support and lipid head-group beads (NC3) are calculated by using equation 2. We did not consider the support beads to interact among themselves.

$$\varepsilon_{SS} = \frac{\varepsilon_{SW}^2}{\varepsilon_{WW}^2} \quad (1)$$

$$\varepsilon_{NC3S} = \sqrt{\varepsilon_{SS} \times \varepsilon_{NC3.NC3}} \quad (2)$$

Where ε_{SW}, ε_{SS} and ε_{NC3S} are the interactions between support-water, support-support and support-lipid head-groups respectively.

The hydrophobicity of the support here is defined in terms of interaction parameter between support with water beads. The interaction strength computed from combining (using geometric mean) epsilons for support and tail beads is relatively lesser than of support and water beads (see Table 1). Therefore, the support favors interacting with water than lipid tail beads. As a consequence of the choice if parameters in this work we did not observe the formation of lipid monolayer on hydrophobic surface. Therefore, it is evident that the hydrophobic supports we have considered in this work can not be termed as super-hydrophobic[52–57] rather moderately hydrophobic with respect to water. Therefore, as a test case we have performed simulations with support and lipid tail beads interaction higher than support water bead(Table S1), which resulted in formation of monolayer on the support (see Figure S2).

2.1 Simulation details

We have constructed the support with completely fixed beads positioned on a square grid of 0.3 nm for the droplet and self-assembly simulations. The X and Y dimensions of the support were carefully chosen to commensurate the resultant surface area of the self-assembled DPPC bilayer. The equilibrium area per headgroup (*APL*) of free-standing DPPC bilayer is 62.4 Å^2. Therefore, considering this, we have chosen box dimension of 12.9 nm$\times$12.9 nm (including 0.3 nm to avoid superimposition of support beads due to periodic boundary condition) along the X and Y directions to accommodate 512 DPPC molecules to form bilayer.

It is observed that, the freezing temperature of coarse grained martini water is higher compared to the real water (or atomistic water) and it freezes rapidly when simulated with solid surfaces.[58] The surface acts as a nucleation site which drives the rapid freezing of coarse grained water near the surface. To tackle such situations, Marrink *et al.* introduced an extra bead called anti-freeze particle (BP4) in the force field to prevent the freezing of water.[50] These beads interact (because of high σ_{ij} and ε_{ij}) with water beads which disturbs the ordering of coarse grained water beads. However the use of anti-freeze particles were not that promising while dealing with the surfaces as reported by Xing *et al.*.[36] Therefore, they have used the weaker water model proposed by Bennun *et al.*[58]. Bennun *et al.* manually reduced water-water interaction and iteratively tested the relationship between the water-water potential and water freezing. They have found that the scaling of ε_{WW} to 76% of original value prevents the freezing of water and reproduces the properties close to bulk water. However, there are some disadvantages of this weaker water model dealing with bilayer simulation. Lamberg *et al.*[59] recently showed, how the equilibrium area per lipid increases with weaker interactions between water molecules.

For the self-assembly of lipids, we have used the water model proposed by Bennun *et al.*[58] and were able to reproduce the results of free standing lipid bilayer.[36](not shown here). From this simulations, we have calculated the area per headgroup of the free standing bilayer (76.0 Å^2) which is same as reported by Xing *et al.*[36]. Finally the same water-water interaction (i.e. scaled ε_{WW} to 76% of the original value of Martini forcefield) was used for all the self-assembly simulations on eight different supports mentioned before. We have performed self-assembly simulations of lipids starting from randomly placed 512 DPPC lipid molecules

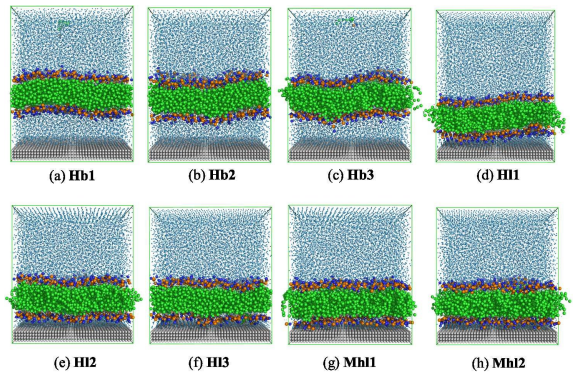

Fig. 2: Final snapshots after the 1μs simulation.

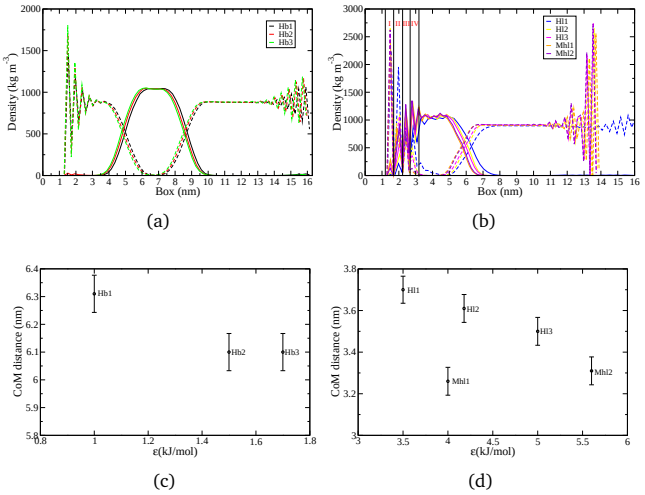

Fig. 3: Partial densities of water (dashed lines) and lipid (solid lines) for a) hydrophobic and b) hydrophilic support system. c) and d) shows the center of mass distance between support and lipid bilayer from hydrophobic and hydrophilic support systems respectively.

on support. Interestingly, we have observed that the system assembled into two distinctly separate lipid domains after 500 ns of the simulation. 456 out of 512 lipids molecules were aggregated together and formed lipid bilayer, whereas, 56 lipids were observed to form a small lipid cluster in a simulation box away from bilayer. Same segregation was observed even by repeating the self-assembly simulation starting from scratch i.e, initial structure (randomly placed DPPC and water molecules). In fact similar trend was observed when we have transferred a well equilibrated free standing lipid bilayer on the support and carried out simulations for 500 ns (Figure S3). The segregation occurred due to the decrease in water density resulting from the 76% scaling of water-water interaction which affects the interfacial tension between lipid-water and the amount of water in the interface. The bilayer was observed to expand to a new equilibrium area per lipid (measured value of 76 Å^2).[36,59]

Henceforth, all the self-assembly simulations on supports were performed with 456 lipid molecules solvated in water starting from a random configuration. The simulations were performed using NAP_zT ensemble by keeping the area constant along the bilayer plane (XY) and constant pressure of 1 bar along z axis. The pressure along Z-axis was controlled by Berendsen barostat. All the simulations were carried out at 323 K which is just above the chain melting temperature of DPPC. The temperature was kept constant by using V-rescale thermostat with temperature scaling factor of 1.5 ps. The cut off for non-bonded Coulombic interaction was r_c = 1.2 nm and the force was smoothly shifted to zero at cut-off. Similarly, the Lennard-Jones potential was shifted smoothly to zero starting from r_s = 0.9 nm. All the systems were simulated for 1 microsecond with a timestep of 15 fs. Self-assembly is a stochastic phenomena. Therefore, the systems were simulated thrice with different initial random configurations of DPPC. Final snapshots of the all these systems are presented in Figure 2. We have developed analysis codes which are described in the results and discussion section.

3 Results and Discussions

3.1 Density profile

We have calculated the partial densities of water and lipid along the bilayer normal (z axis) for all self-assembled systems. The density profiles are plotted separately for hydrophobic and hydrophilic support systems in Figure 3a and b respectively. It is reported that the surface acts as a nucleation site for Martini water beads, which induces water to freeze rapidly near the proximity.[58,60] Therefore, a clear ordering of the coarse grained water near all the support surfaces is observed.

A relatively higher ordering of the water near the hydrophilic than hydrophobic support is observed due to stronger attractive interactions (see Figure 3b). The observed bulk water density $\sim 900 kg/m^3$ (Figure 3a and b) with scaled interactions is in good agreement with work by Xing *et al.*[36] Interesting thing we have noticed is that, the location of the self-assembled bilayer in simulation box is guided by the hydrophobic or hydrophilic nature of the support. In case of the hydrophobic supports, the repulsive interaction between lipid head group and support which resulted into bilayer formation away from the surface. However, the formation of bilayer proceeds due to the contributions from inter-lipid and lipid-water interactions. In case of hydrophilic support, surface beads attract the head group beads of amphiphilic lipid and the formation of bilayer takes place near to the support. We have calculated the center of mass (CoM) distance between the lipid bilayer and support as a function of interaction parameters and depicted in Figure 3c and d. We have observed that the bilayers formation takes place near the hydrophilic support than the hydrophobic, because of the higher attractive interactions between head-groups and the support.

We have also computed two-dimensional density map of water averaged over the Y axis to visualize the density of water across the simulation box. The density maps were calculated from last 50 ns of total 1 μs trajectory. The ordering of water near the surface is clearly visible from Figure 4 and it is also seen from the partial density profiles in Figure 3. However, the density of water near the surface is apparently higher in case of hydrophilic supports compared to the hydrophobic. The hydrophilic solid support enhances water ordering upto ∼2.8 nm (six dense water layers)

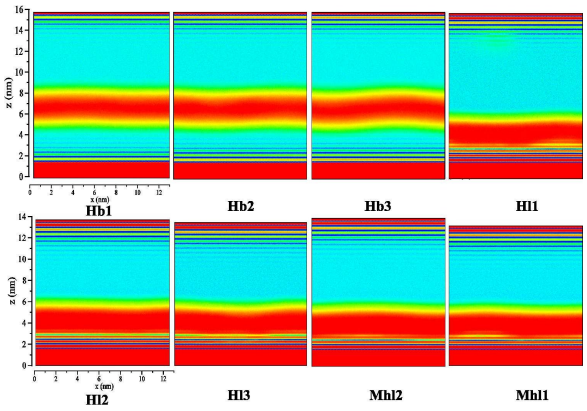

Fig. 4: Two dimensional density map of water.

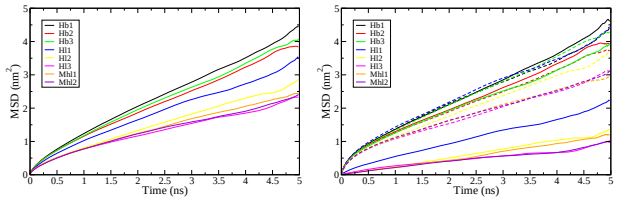

(a) (b)

Fig. 5: a) Mean square displacement (MSD) of lipids. b) MSDs of NC3 beads of lower leaflet lipids as dashed lines whereas NC3 beads from upper leaflet showed as solid lines.

from the surface. The ordered water layers upto ∼1.5 nm are observed for hydrophobic supports but are less denser compared to hydrophilic supports which is also noted from the partial density plots (Figure 3).

3.2 Diffusion

It is observed that lipid molecules in a supported bilayer system show slower diffusion as compared to the unilamellar vesicles.[61] Thus, we have examined the dynamics of the lipid molecules by calculating mean squared displacement (MSD) of CoM of each lipid molecule. Figure 5a, shows the average MSD computed at an interval of 5 ns each from last 50 ns trajectory (the lipids are already in self-assembled bilayer form). From this figure (Figure 5a), it is evident that the diffusion of the lipid is strongly affected in case of hydrophilic supports. The attractive force from the support significantly reduces the mobility of lipids. We have also observed that the strength of hydrophilicity of the support has an effect on the lipid mobility. From the diffusion coefficient values provided in Table S2 and MSD plots (Figure 5), it is clear that hydrophilic supports Hl3 and Mhl2 can slow down the dynamics of lipid molecules by ∼50 % of any hydrophobic system. However, by construction Hl1 system is a border line between hydrophobic and hydrophilic support, so it is evident that the decrease in diffusion is not much.

The lower leaflet (i.e. near to the support) of self-assembled bilayer on support interacts more with the surface beads than outer leaflet. Therefore, we have investigated the effect of hydrophilicity on lipid leaflets separately. The MSD of the lipid head-group beads (NC3) are calculated based on the leaflets. Figure 5b depicts the leaflet-wise averaged MSD from 5 ns time interval as a function of time. The diffusion coefficients computed from the slope (linear region) are listed in Table S2. The lower leaflets of hydrophilic supports are severely slowed down because of higher interaction than the upper leaflets. We can even observe significant arrest of motion of lipid headgroups for Hl1 support. Both, Hl3 and Mhl2 supports exhibit ∼80% decrease in diffusion of headgroups (NC3). Interestingly, we do not observe any significant effect of the hydrophobic surface on the diffusion of headgroups either in lower or upper leaflet of the bilayer.

3.3 Lipid order

Lipid tail order parameter is a measure of lipid ordering and their packing in the bilayer. Bilayer properties, such as fluidity, which is dependent on ordering of lipid tail. The order parameters for coarse grain lipid beads used in our simulations can be calculated by the following equation.

$$P2 = 0.5 \times (3 \times < cos^2(\theta) >) - 1 \quad (3)$$

where θ is the angle between the bonds of two adjacent beads and bilayer normal. The value of P2=1 denotes the perfect alignment of the lipid with the bilayer normal, P2=-0.5 is anti-alignment and P2=0 represents random orientation of lipid beads.

We have calculated the order parameters of self-assembled lipids both on hydrophilic and hydrophobic supports and plotted in Figure 6a. In Figure 6a black line denotes the lipid tail order parameter for a free standing lipid. We have plotted average lipid tail order parameters separately for upper (red dashed line) and lower leaflet (red solid line) i.e., the layer near to the support. The numbering in the x-axis (of Figure 6a) denotes the bond number connecting consecutive tail beads. The number 1 denotes the bond which is connecting the Glycerol moiety to the next nearest bead (Figure 6b)(e.g. bond 1 is GL1-C1A) and 4 is the farthest. In case of hydrophobic support, we did not observe a significant change from free standing lipid, which may be obvious, as the self-assembly happens at a larger distance from the support compared to hydrophilic support.

However, for hydrophilic support, the upper leaflet of all the systems (except Hl1) gets affected and their ordering gets increased. Hl1 is the border line case, where hydrophilicity of support is not as much as other systems, thus the upper leaflet is almost free from any interaction due to the support and show similar trend as free standing lipid. We have observed a significant differences in ordering of the upper and lower leaflet with the increase in the hydrophilic nature of the support (e.g., Hl2, Hl3, Mhl1, Mhl2). Because of interaction with support and water beads, the lower leaflet is mostly less ordered than the upper leaflet. Even for the most hydrophilic systems (i.e., Hl3 and Mhl2), the ordering of lower leaflet crosses the free standing lipid. It is interesting to observe that the surface hydrophilicity enhances the ordering of the leaflet which is not interacting (upper leaflet) and decreases the ordering of the interacting leaflet.

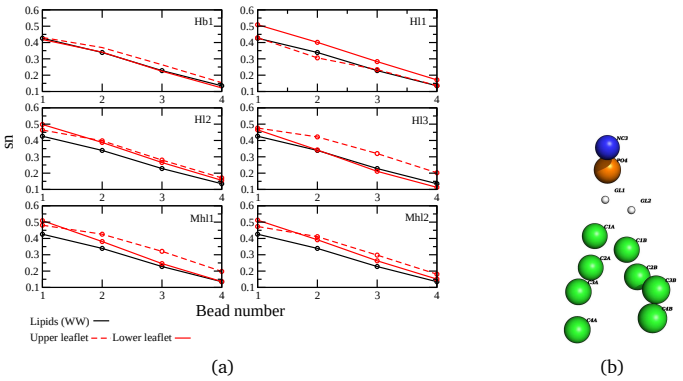

Fig. 6: a) Lipid order parameters. Black solid line represents free standing lipid tail order parameters and red dotted and solid lines are upper and lower leaflet of supported bilayers b) schematic representation of DPPC lipid.

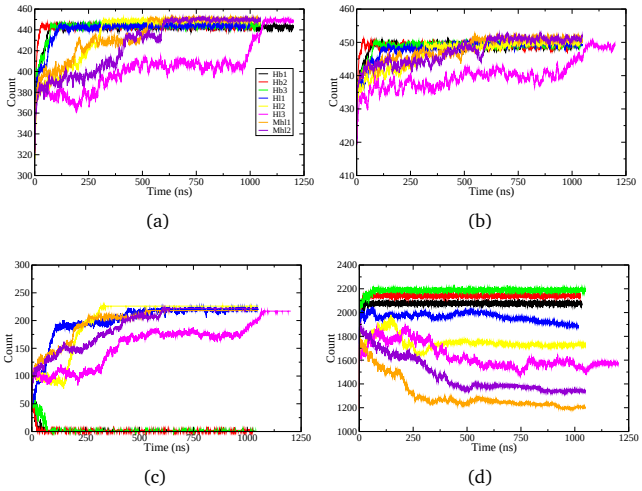

Fig. 7: Number of beads within 0.9 nm distance cut-off of intra a) NC3 bead and b) C1 beads distances as a function of simulation time. Figure c and d shows the number of NC3 and W beads near the support respectively.

3.4 Mechanism of self-assembly

Self-assembly is a random chemical process that involves with the arrangement of molecules from a disordered state to an organized macroscopic structure or pattern. In lipid self-assembly, lipids arrange themselves together to form lammellar, micelle or vesicular structures depending on the chemical environment, composition and concentration. It is a result of hydrophobic interactions along the lipid tails, as they try to minimize the contact with aqueous solvent and lipid headgroups pointing outside facing water molecules. During the self-assembly of lipids, it is expected that the hydrophobic interactions bring lipid tails (C1 beads) together and the hydrophilic interaction drives NC3 beads (lipid head groups) to come closer. In the present study, we focus on the self-assembly of the lipids in presence of supports as a function of simulation time by checking the proximities of hydrophilic and hydrophobic entities. From the trajectory, we have calculated the number of NC3 beads coming in contact with each other as a function simulation time. We have calculated inter NC3 bead distances and counted the number of beads within 0.9 nm cut-off. This cut-off mainly takes care of the DPPC area per head-group (76 $\AA^2$) and counts the adjacent lipids.

In Figure 7a, we have plotted this count as a function of time which shows a significant difference in case of lipid which are on hydrophilic support. Similarly, to quantify the collapse due hydrophobic interactions, we have computed the number of lipid tail (terminal C1 beads) coming together as a function of time. We have used the same cutoff of 0.9 nm to calculate the count (see Figure 7b). From Figure 7a and b, it is evident that in case of Hb1, Hb2 and Hb3 systems, lipids self-assemble within initial few nanoseconds (∼20-80 ns) (Figure S4). Both head and tail group lipid beads have come together in a similar time frame. On the contrary, self-assembly of lipid beads have taken longer time on hydrophilic supports. In case of Hl3 system, the lipid molecules taken the longest time ∼1000 ns to get settled on the support surface. This essentially occurs due to the competitive forces acting among the support, water and lipid.

The repulsive or the attractive interaction from the support can assist or delay the self-assembly process. However, in all cases we have observed self-assembly. Now, it was important to understand the interplay between the interactions of lipid and water with the support. The question was, how these inter-particle forces guide the self-assembly of lipids? For that, we have calculated the number of lipid head-groups (NC3) and water beads in the close vicinity of the support as a function of simulation time. We have taken a cut-off of 2.5 nm (from the first layer of surface beads), because the location of the bilayer-water interface from the support surface (see Figure 3) falls within that range. The NC3 and water bead counts as a function of time plotted in Figure 7c and d respectively. As we have started the simulation from randomly distributed molecules we have observed clearly that in case of Hb1, Hb2 and Hb3 supports, the NC3 beads move away from the surface and count reaches to zero in a very short time span of $\sim 20-80$ ns. On the other hand, hydrophilic supports induces the lipid molecules to settle down near all the surfaces due to attractive interactions.

The hydrophilic support imparts a strong interaction towards water beads. It is evident from Figure 7d that, there is a decrease in the number of water beads near hydrophilic support. This might be possible because head-groups (NC3) also favor to interact with hydrophilic support beads. As a result, NC3 beads get accumulated near hydrophilic support competing with water. However, from the 2-dimensional density maps (Figure 4), we have seen that the density of water near to the surface is higher in case of hydrophilic support than hydrophobic support. In the hydrophilic support systems, the interaction potentials ε_{SW} are more attractive than ε_{NC3S} (Table 1), therefore water beads settle more in number near to the support surface. Besides that, the support acts as a nucleation site, thus, favors waters bead to arrange near the surface. However, approximately within 2.5 nm (see Figure 3 for the partial density of water near hydrophilic support) from the hydrophilic support, there is a competition between lipids and water for finding the position after the initial deposition of the water adjacent to the support. However apart

from this, there are also inter-particle interactions other than surface contributing to the lipid self-assembly. It includes inter-lipid, lipid-water and water-water beads interactions. E.g., in Hl1 system, the support beads interact with water with ε_{SW} = 3.5 kJ/mol, water-water interaction strength is ε_{WW} = 3.8 kJ/mol. Further, the nucleation of the water allows these interactions to overcome the support-head group (ε_{NC3S} = 2.92 kJ/mol) (see Table 1) and hence accelerates water beads to settle near support surface. Beyond the non-bonded cut-off from support, we have found ε_{NC3W} interactions dominate which helps in the self-assembly process. Therefore, we have observed a sharp rise in the NC3 count for all hydrophilic support (Figure 7c).

However, it was still unclear that, why the number of water molecules near hydropholic support (expect Hl1 system) decreases with time even though the water densities are higher near hydrophilic supports (2.5 nm from the support surface). Apparently for hydrophobic support systems, we have observed a higher number of water beads resides in the 2.5 nm cut-off from support surface. This mainly resulted due to the formation of bilayer that takes place away from the support. Interestingly, the number of water beads gradually increases with the interaction parameters (ε_{SW}) for hydrophobic support with water. The water density increases as the support attracts more water with increase in hydrophilicity.

To address the anomaly of the lesser water bead count near hydrophilic supports (Hl2, Hl3, Mhl1 and Mhl2) compared to hydrophobic support. We have calculated the partial densities of water and head-group beads (NC3) near the hydrophilic support (within the cutoff of 2.6 nm). As the amphiphilic lipids are settling down near the surface, it is expected that lipids may be replacing some of the water beads. In figure 8, we have plotted the partial density of the water and NC3 groups during self-assembly (i.e. initial 0 - 50 ns) with an interval of 10 ns.

The 1st layer of water has a higher density than other layers for all the hydrophilic systems. However, the number of water beads in the second and third layers varies and we have observed a significant number of NC3 beads have penetrated these two water layers. This is because of favorable water - NC3 bead interaction parameter and competition between water and NC3 bead to settle down near the surface. Thus, we have seen lesser water bead count in proportional to the hydrophilicity of the support. The maximum density of NC3 is noted in Mhl1 system due to the competitive interactions between NC3 and W with support (ε_{NC3N}=ε_{SW} = 4 kJ/mol).

Self-assembly is a stochastic phenomena. Therefore, we have carried out three independent self-assembly simulations starting from random configurations. In Figure S5 of ESI, we depicted the results from the second set of self-assembly simulation. From Figure S5, we have observed a similar trend in self-assembly process for the all the systems except Hl2 which took longer time to self-assemble. The delay in the self-assembly is due to the competitive interactions ε_{NC3S}= ε_{C1S}= ε_{C1C1}= 3.5 kJ/mol (see Table 1) between support and lipid beads.

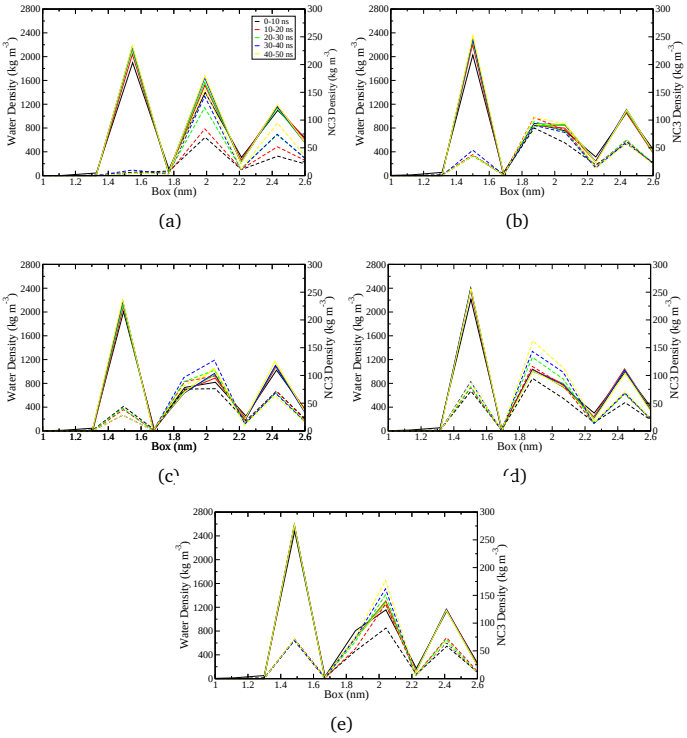

Fig. 8: Partial densities of water (solid lines) and NC3 beads (dashed lines) as a function of time interval of 10 ns each. a, b, c and d represents system Hl2, Hl3, Mhl1 and Mhl2 respectively.

3.5 Energetics of the mechanism

We have further examined these systems by calculating the potential energy, i.e., non-bonded Lennard Jones (LJ) interaction energies experienced by lipid-head group and water beads separately in different regions near to the support surface. In case of hydrophilic support we have observed the self-assembly of lipids near to the support. Therefore, here we have only reported the energies related to the hydrophilic support systems. We have observed a competition between the lipid head-groups and water beads for finding a position predominately within the distance of 2 nm from the support surface. The partial densities (Figure 3) also evident that, this region is the most oscillating region where water and headgroup beads are getting arranged. Hence, we have divided this region in four equal slabs (denoted as I, II, III and IV region) of 0.5 nm staring from 1.2 nm to 3.2 nm (see Figure 3). In these predefined regions (of self-assembled equilibrated), we have calculated the total energy (sum of non-bonded energy between water/headgroup and all other beads) by each water and headgroup bead. The energies in different regions are further plotted as a distribution in Figure 9.

From this Figure (right panel), it is evident that water is the most energetically favored near to the surface (region I) and then in region II. As Hl3 and Mhl2 are the most hydrophilic systems in two categories, water near to these surfaces (in region I) are energetically favorable. However, as we go further from the surface, i.e., in region II, III and IV the potential energy experienced by water of different support hydrophilicity are almost similar (overlapping distributions). However, in case of headgroup beads

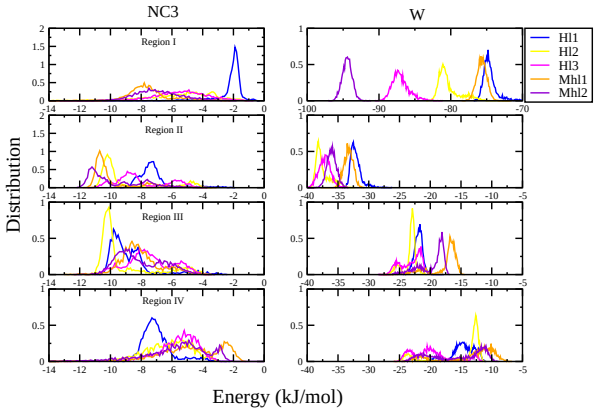

Fig. 9: Potential energy (LJ) between the beads near hydrophilic supports. Left and right panels shows energies felt by water and NC3 beads respectively in different regions.

(NC3) the region II and III are the more energetically favorable regions. In region II and III headgroup beads get stabilized by interacting with water and support beads. The separate energy contributions to the total energy of headgroup in these regions are given in Figure S6 and S7. It is also evident from Figure 9 that in region II and III there are not much influence of the support on headgroup beads. In region II most hydrophilic support (Mhl2) marginally stabilizes the headgroup beads, but in region III less hydrophilic support (Hl1, Hl2) stabilize the headgroups. In region III and IV of Figure 9 we observe the broad distribution of energies felt by headgroups due to varied balancing interactions from water, surface and lipid tails beads. This is one of the main reasons why we observe less ordering in lipid tail (see Figure 6).

These observations confirm that the lipid self-assembly with the solid supports mainly guided by the various interactions taking place between the support, lipids and water beads. The arrangement of molecules from disordered state into organized macroscopic structures is predominantly dependent upon the properties of the support and nature of the interacting particles.

4 Conclusions

We have carried out the lipid self-assembly simulations on different model supports constructed on the basis of their hydrophobic or hydrophilic nature. Significant differences are noticed in all these self-assembly processes. The hydrophobic support, due to the repulsive interaction, repels the lipids and the bilayer formation observed at a distant region from the support. The lipid bilayers settle down near to the modeled hydrophilic support due to favorable attractive interactions. We have found out that the lipid bilayers from the hydrophobic support systems were least affected, whereas, the hydrophilicity of the support affects the bilayer properties to a certain extent. The ordering of lower and upper leaflets is affected in case of hydrophilic support. The hydrophilic supports are found to enhance the water ordering near the support as evident from the structural and dynamical properties of water. During the self-assembly, hydrophobic supported lipids arrange quickly to form lipid bilayer whereas the hydrophilic support delays the self-assembly process. It is mainly because of the interplay between surface-head, head-head, surface-water and head-water interactions. We confirmed the competition between water and lipid head-group to interact with hydrophilic supports by calculating energetic of the system.

Acknowledgements

Author Anil R. Mhashal would like to thank CSIR-UGC, India for providing the fellowship. Author Sudip Roy gratefully acknowledges center for Excellence in Scientific Computing, NCL (project code CSC0129), for a computational time.

References

1 E. Sackmann, *Science*, 1996, **271**, 43–48.
2 B. A. Cornell, V. L. B. Braach-Maksvytis, L. G. King, P. D. J. Osman, B. Raguse, L. Wieczorek and R. J. Pace, *Nature*, 1997, **387**, 580–583.
3 J. T. Groves and M. L. Dustin, *Journal of Immunological Methods*, 2003, **278**, 19 – 32.
4 I. Czolkos, A. Jesorka and O. Orwar, *Soft Matter*, 2011, **7**, 4562–4576.
5 E. Tanaka, M.; Sackmann, *Nature*, 2005, **437**, 656–663.
6 E. T. Castellana and P. S. Cremer, *Surface Science Reports*, 2006, **61**, 429 – 444.
7 B. N. Manz, B. L. Jackson, R. S. Petit, M. L. Dustin and J. Groves, *Proceedings of the National Academy of Sciences*, 2011, **108**, 9089–9094.
8 N. C. Hartman, J. A. Nye and J. T. Groves, *Proceedings of the National Academy of Sciences*, 2009, **106**, 12729–12734.
9 S. Pautot, H. Lee and J. T. Isacoff, E. Y.and Groves, *Nature Chemical Biology*, 2005, **1**, 283–289.
10 K. Salaita, P. M. Nair, R. S. Petit, R. M. Neve, D. Das, J. W. Gray and J. T. Groves, *Science*, 2010, **327**, 1380–1385.
11 T. LohmÃijller, S. Triffo, G. P. OâĂŹDonoghue, Q. Xu, M. P. Coyle and J. T. Groves, *Nano Letters*, 2011, **11**, 4912–4918.
12 A. Rumpel, M. Novak, J. Walter, B. Braunschweig, M. Halik and W. Peukert, *Langmuir*, 2011, **27**, 15016–15023.
13 Y. K. Lee and J.-M. Nam, *Small*, 2012, **8**, 832–837.
14 R. P. Richter, R. BÃľrat and A. R. Brisson, *Langmuir*, 2006, **22**, 3497–3505.
15 I. Reviakine and A. Brisson, *Langmuir*, 2001, **17**, 8293–8299.
16 C. Larsson, M. Rodahl and F. HÃűÃűk, *Analytical Chemistry*, 2003, **75**, 5080–5087.
17 I. Reviakine, W. Bergsma-Schutter and A. Brisson, *Journal of Structural Biology*, 1998, **121**, 356 – 361.
18 A. A. Brian and H. M. McConnell, *Proceedings of the National Academy of Sciences*, 1984, **81**, 6159–6163.
19 P. Lenz, C. M. Ajo-Franklin and S. G. Boxer, *Langmuir*, 2004, **20**, 11092–11099.
20 S. Goennenwein, M. Tanaka, B. Hu, L. Moroder and E. Sackmann, *Biophysical Journal*, 2003, **85**, 646 – 655.
21 M. L. Wagner and L. K. Tamm, *Biophysical Journal*, 2001, **81**, 266 – 275.
22 J. C. Munro and C. W. Frank, *Langmuir*, 2004, **20**, 10567–10575.

23 V. I. Silin, H. Wieder, J. T. Woodward, G. Valincius, A. Offenhausser and A. L. Plant, *Journal of the American Chemical Society*, 2002, **124**, 14676–14683.

24 S. Terrettaz, M. Mayer and H. Vogel, *Langmuir*, 2003, **19**, 5567–5569.

25 O. Purrucker, A. FÃűrtig, R. Jordan and M. Tanaka, *ChemPhysChem*, 2004, **5**, 327–335.

26 W. RÃűmer, Y. H. Lam, D. Fischer, A. Watts, W. B. Fischer, P. GÃűring, R. B. Wehrspohn, U. GÃűsele and C. Steinem, *Journal of the American Chemical Society*, 2004, **126**, 16267–16274.

27 W. RÃűmer and C. Steinem, *Biophysical Journal*, 2004, **86**, 955 – 965.

28 S. Svedhem, I. Pfeiffer, C. Larsson, C. Wingren, C. Borrebaeck and F. HÃűÃűk, *ChemBioChem*, 2003, **4**, 339–343.

29 C. Yoshina-Ishii and S. G. Boxer, *Journal of the American Chemical Society*, 2003, **125**, 3696–3697.

30 M.-P. Mingeot-Leclercq, M. Deleu, R. Brasseur and Y. F. Dufrene, *Nature Protocols*, 2008, **3**, 1654–1659.

31 J. T. Groves, N. Ulman and S. G. Boxer, *Science*, 1997, **275**, 651–653.

32 K. C. Weng, J. J. Stalgren, S. H. Risbud and C. W. Frank, *Journal of Non-Crystalline Solids*, 2004, **350**, 46–53.

33 E. Kalb, S. Frey and L. K. Tamm, *Biochimica et Biophysica Acta (BBA) - Biomembranes*, 1992, **1103**, 307 – 316.

34 L. Tamm and H. McConnell, *Biophysical Journal*, 1985, **47**, 105 – 113.

35 T. Charitat, E. Bellet-Amalric, G. Fragneto and F. Graner, *The European Physical Journal B - Condensed Matter and Complex Systems*, 1999, **8**, 583–593.

36 C. Xing and R. Faller, *The Journal of Physical Chemistry B*, 2008, **112**, 7086–7094.

37 J. Yang and J. Appleyard, *The Journal of Physical Chemistry B*, 2000, **104**, 8097–8100.

38 D. Keller, N. B. Larsen, I. M. Møller and O. G. Mouritsen, *Phys. Rev. Lett.*, 2005, **94**, 025701.

39 A. Charrier and F. Thibaudau, *Biophysical Journal*, 2005, **89**, 1094 – 1101.

40 Z. V. Feng, T. A. Spurlin and A. A. Gewirth, *Biophysical Journal*, 2005, **88**, 2154 – 2164.

41 S. Stanglmaier, S. Hertrich, K. Fritz, J.-F. Moulin, M. Haese-Seiller, J. O. RÃď dler and B. Nickel, *Langmuir*, 2012, **28**, 10818–10821.

42 A. P. Shreve, M. C. Howland, A. R. Sapuri-Butti, T. W. Allen and A. N. Parikh, *Langmuir*, 2008, **24**, 13250–13253.

43 F. F. Rossetti, M. Textor and I. Reviakine, *Langmuir*, 2006, **22**, 3467–3473.

44 T. Cha, A. Guo and X.-Y. Zhu, *Biophysical Journal*, 2006, **90**, 1270 – 1274.

45 X. Lin, C. Wang, M. Wang, K. Fang and N. Gu, *The Journal of Physical Chemistry C*, 2012, **116**, 17960–17968.

46 H. Lee and H. Kim, *The Journal of Physical Chemistry C*, 2012, **116**, 9327–9333.

47 H. Berendsen, D. van der Spoel and R. van Drunen, *Computer Physics Communications*, 1995, **91**, 43–56.

48 B. Hess, C. Kutzner, D. van der Spoel and E. Lindahl, *Journal of Chemical Theory and Computation*, 2008, **4**, 435–447.

49 S. J. Marrink, A. H. de Vries and A. E. Mark, *The Journal of Physical Chemistry B*, 2004, **108**, 750–760.

50 S. J. Marrink, H. J. Risselada, S. Yefimov, D. P. Tieleman and A. H. de Vries, *The Journal of Physical Chemistry B*, 2007, **111**, 7812–7824.

51 S. J. Marrink and D. P. Tieleman, *Chem. Soc. Rev.*, 2013, **42**, 6801–6822.

52 J.-W. Park and G. U. Lee, *Langmuir*, 2006, **22**, 5057–5063.

53 J. S. Li, E. Ueda, A. Nallapaneni, L. X. Li and P. A. Levkin, *Langmuir*, 2012, **28**, 8286–8291.

54 M. Shaali, S. Lara-Avila, P. Dommersnes, A. Ainla, S. Kubatkin and A. Jesorka, *ACS Nano*, 2015, **9**, 1271–1279.

55 B. Sanii and A. N. Parikh, *Soft Matter*, 2007, **3**, 974–977.

56 J. T. Elliott, D. L. Burden, J. T. Woodward, A. Sehgal and J. F. Douglas, *Langmuir*, 2003, **19**, 2275–2283.

57 S. Lingler, I. Rubinstein, W. Knoll and A. OffenhÃď usser, *Langmuir*, 1997, **13**, 7085–7091.

58 S. V. Bennun, A. N. Dickey, C. Xing and R. Faller, *Fluid Phase Equilibria*, 2007, **261**, 18 – 25.

59 A. Lamberg and T. Taniguchi, *The Journal of Physical Chemistry B*, 2014, **118**, 10643–10652.

60 P. Kumar, S. V. Buldyrev, F. W. Starr, N. Giovambattista and H. E. Stanley, *Phys. Rev. E*, 2005, **72**, 051503–051514.

61 M. Przybylo, J. SÃikora, J. HumpolÃ■Ä■kovÃą, A. Benda, A. Zan and M. Hof, *Langmuir*, 2006, **22**, 9096–9099.